Summer 8-2020

Exploration of the Relationship Between the Fractal Dimension of Microcalcification Clusters and the Hurst Exponent of Background Tissue Disruption in Mammograms

Betelhem Abay

EXPLORATION OF THE RELATIONSHIP BETWEEN THE FRACTAL DIMENSION OF MICROCALCIFICATION CLUSTERS AND THE HURST EXPONENT OF BACKGROUND TISSUE DISRUPTION IN MAMMOGRAMS

by

Betelhem S. Abay

A Thesis Submitted in Partial Fulfillment
of the Requirements for a Degree with Honors
(Biomedical Engineering)

The Honors College

University of Maine

August 2020

Advisory Committee:

Andre Khalil, Associate Professor of Chemical and Biomedical Engineering, Advisor
Paula Drewniany, Lecturer of Mathematics and Statistics
Christopher Mares, Honors Preceptor and Lecturer in English as a Second Language
Karissa Tilbury, Assistant Professor of Chemical and Biomedical Engineering
Brian Toner, Ph.D. Candidate in Computer Science

ABSTRACT

Breast cancer is one of the most frequent cancers among women worldwide and holds the second place in cancer-related death. Mammography is the most commonly used screening technique, however, the dense nature of some breasts makes the analysis of mammograms challenging for radiologists. The 2D Wavelet Transform Modulus Maxima (WTMM) is one mathematical approach that is used to for the analysis of mammograms. In 2014, a team from the CompuMAINE Lab characterized differences between benign microcalcification clusters (MC) from malignant MC by calculating their fractal dimension, *D,* with the aid of the 2D WTMM method. In a different implementation of the 2D WTMM method, this same team did research in 2017 where they quantified tissue disruption in breast tissue microenvironment using the Hurst exponent, *H*. The goal of this study was to further explore the potential relationship between the fractality of MC clusters and tissue disruption in the microenvironment surrounding these clusters. Statistical relationships are explored between the fractal dimension, *D*, of MC clusters and the Hurst exponent, *H* measuring tissue disruption. A "2D fractal dimension vs. Hurst exponent plot" was graphed to show this relationship used to distinguish between benign and malignant cases. In the graph, a quadrilateral region extending horizontally from Hurst value of (0.2,0.8) centered at 0.5 and stretching vertically from fractal dimension value of (1.2,1.8) centered 1.5 was identified. Analysis of this region has showed that the 60% of the malignant cases and 21% benign cases are found inside the quadrilateral for CC view and 68% of the malignant cases and 12% of benign cases are found inside the region for MLO view. As a conclusion, based on the outcomes of this study one can hypothesize that with further analyses, loss of tissue homeostasis describing the state of the microenvironment of a

breast tissue and the fractal nature of MC clusters have a quantifiable relationship to distinguish benign cases from malignant cases in mammogram analysis.

ACKNOWLEDGEMENTS

First and foremost, praises and thanks to God, the Almighty, for His showers of blessings support throughout my research work to complete the research successfully.

I would like to express my deep and sincere gratitude to my research advisor, Prof. Andre Khalil for giving me the opportunity to do this research in his lab, for his valuable guidance throughout the study, and for sharing his knowledge in every aspect. I would like to thank Christopher Mares for his consistent support to help me improve my writing in English since I joined the Honors college and now for his guidance in structuring and formatting my reading list. I would like to thank all my other thesis committee members Prof. Karissa Tilbury, lecturer Paula Drewniany, and Brian C. Toner for supporting me and providing me with valuable input and feedback for my research. I would also like to extend my gratefulness to the University of Maine Writing Center for their consistent support in my thesis writing.

I am extremely grateful to my parents for their love, prayers, caring and sacrifices for educating and preparing me to my future. I am very much thankful for all my extended family members in New Jersey, my brother, my cousins, and my best friend for their continuous support throughout my study abroad. A special thanks and respect to the Norman's and Bob Mowdy's family for being a second family and giving me a home away from home. Also, I would like to express my appreciation to all the University of Maine community for helping me grow as an individual, as a leader, and as an engineer.

TABLE OF CONTENTS

LIST OF FIGURES

CHAPTER 1: INTRODUCTION

Breast cancer is one of the most common diseases around the world that affects many families' lives. If caught early, breast cancer can be treated before further complications occur. Most of the current existing breast imaging techniques include magnetic resonance imaging (MRI), ultrasound, and mammography (low energy x-rays). Ultrasound and mammography imaging are the two most common techniques used to screen breast cancer. MRI is a more sensitive method of breast screening and unlike the other two methods, it is virtually uninfluenced by breast density, but it is expensive.[1–4] Computer-aided diagnostics (CAD) are systems that were invented to assist doctors with the interpretation of medical images (like breast images) and have been in application for several years. Since these CAD techniques have been approved by the FDA, the rate at which malignant tumors or suspicious cancer zone identification such as microcalcification detection has shown a potential increase by approximately 20%.[5] This statistics is based on the recall rates for mammogram analysis with and without CAD by experienced radiologists. Most developed countries like the US use these technologies to assist radiologists in interpreting mammography images, which eases their job and also gives a better insight into suspicious (cancerous) regions.[5] However, this widely used technology has unfortunately been associated with false diagnostics. Improving the efficiency of analyzing images using these CAD techniques is crucial in minimizing the morbidity and mortality rate of cancer around the world.

Some of the factors that could lower the sensitivity of mammography include technical and interpretative errors, rapid tumor growth and its patterns, and extensive mammographic breast density.[6] The breast tissue microenvironment plays an important

role in the growth of malignant or benign tumors. Developing a quantitative support for a mathematical interpretation of the breast microenvironment could help in understanding the different patterns and progression of tumor 2growth. The concept of fractal geometry is one mathematical approach that could be applied to solve this difficulty in breast image interpretation. Fractal geometry is a tool that is used to study objects with irregular geometry (non-integer values of dimension *D*), rather than the regular 1-D, 2-D, or 3-D geometries mostly referred as Euclidean objects (integer values of dimension *D*).[7] The fractal dimension, *D*, refers to the exponent in the power-law relationship between the number of balls required to cover a set, *N,* and the radius of the balls, *r*, i.e. $N \sim (1/r)^D$ as shown in Figure 1. Previous mathematical studies have shown that benign tumors have a Euclidean geometry form of growth whereas malignant tumors follow the fractal geometry form of growth.[7,8] The fractal growth nature of the malignant tumors can be used to create a fractal-based background model of breast tissue in order to find calcification clusters.[9–11]

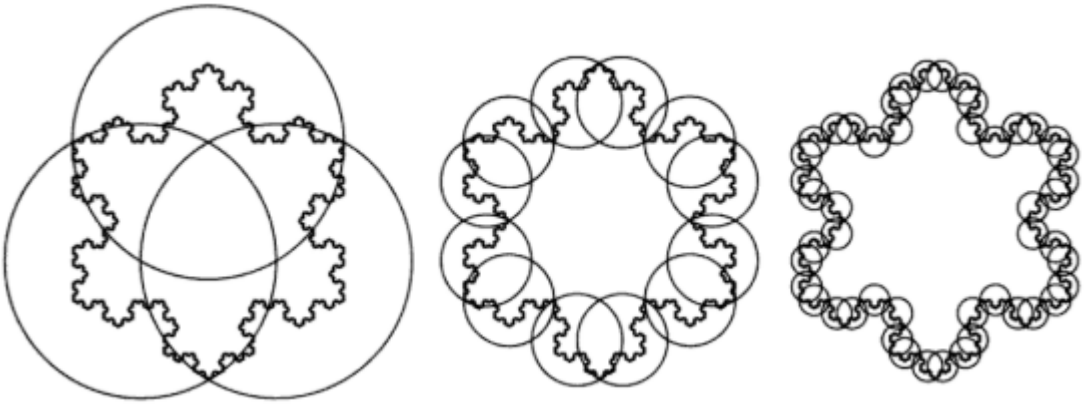

Figure 1: Different radii balls covering the perimeter of Koch's island.
Adopted from Ref. [12]

Breasts are organs with a very dense tissue composition with mostly fatty tissue and some fibrous and glandular tissues. Although the source is not clearly known, the lactation ducts in the breast can start having calcium deposits that cluster in two main,

different ways. These calcification clusters are divided into macrocalcification clusters (mainly associated with benign tissues) and microcalcification (MC) clusters (mainly associated with malignant tissues). Calcification clusters are major and very important when looking at a mammography image, (mammograms) as they are suspected to be regions of malignant tumors. Previous research has been conducted on the geometry of microcalcifications by the CompuMAINE Lab, at the University of Maine, by studying the fractal dimension of MC clusters. The outcome of the study is that benign breast lesions were identified to have a fractal dimension, *D* of 1 or 2 (Euclidean dimension) but malignant breast lesions have *D* closer to 1.5 (i.e. a non-integer, fractal dimension).[7] A different research conducted by this same team studied the architecture of breast microenvironment by using the Hurst exponent, *H*, as a quantifying index.[13] In that study they showed evidence that tissue disruption and loss of homeostasis in breast tissue microenvironment and breast bilateral asymmetry can be quantitatively assessed from mammography using a wavelet analysis of the whole breast. The outcome from that study has shown a potential for the development of a metric that can study the biophysics of loss of tissue homeostasis and breast tissue disruption that enhances the possibility for early identification of potential danger zones.

The development of a more reliable and valuable quantitative assessment methodology based on fractal geometry could assist in mammography interpretation, leading to an improved cancer detection accuracy. In this project the mathematical calculations for *H* and *D* from mammograms previously analyzed with the aid of the 2D Wavelet-Transform Modulus Maxima (WTMM) method were made available by the CompuMAINE Lab. The goal of this project is to explore potential correlations between

the fractality of the breast tumors (MC clusters) and the state of tissue homeostasis of the microenvironment surrounding these tumors. To do so, we investigated statistical relationships between the fractal dimension of MC clusters (*D)* and microenvironment tissue disruption as measured by the Hurst exponent, *H.* Based on the outcomes from the 2014 and the 2017 studies, it is expected that this statistical analysis is going to show a significant relationship between the Hurst exponent and the fractal dimension.

CHAPTER 2: BREAST ANATOMY AND CALCIFICATION

2.1 Normal Anatomy and Physiology

The breast is located on the upper ventral region of the torso in primates. Breasts start to develop in the first five weeks of the human fetus, as the mammary ridge starts to develop on either side from the axilla to the groin. The axilla contains the vessels and nerves of the upper extremity. Breasts are composed of different tissue layers mainly of glandular (secretory) tissues and adipose (fatty) tissues surrounded by a loose framework of fibrous connective tissues called Cooper's ligaments. The human breast reaches its full functional capability when it develops enough glandulars for lactation (milk secretion) which also acts as a means of communication between the baby and the mother.[14] The mammary glands of the breast always find a way to secrete or continuously supply calcium in order to concentrate the milk with the needed amount of calcium. However, a large amount of calcium is toxic to cells, therefore the mammary epithelial cells have to find a way to transport large amounts of calcium to extracellular fluid, through their cytoplasm into the milk.[15] The large amount of calcium that leaves the mother results in mobilization of skeletal calcium and a reduction in bone mass.[15,16] Throughout this whole process, calcium is transported through the milk ducts of the breast.

2.2 Calcification of the Breast

Calcium is one of the most important minerals in our body and it needs to be tightly regulated. Calcium is found in the blood, muscles, and other tissues. It is essential for the growth of strong teeth and bones, for heart function, blood clotting, nerves, and many other functions in the human body. Calcium is also found in the dense tissue of the breast. This

mineral circulates in blood serum which is part of the blood plasma that does not contain blood cells. Serum calcium is mostly controlled by calcium itself through different calcium receptors and the two hormones: parathyroid hormone (PTH) and $1,25(OH)_2$ vitamin D.[17] As PTH increases with age, its overproduction is suspected to be a risk for breast cancer.[18] In a research conducted to study if calcium in blood serum is a risk factor for breast cancer in women at pre/post menopause, it was found that a single measurement of serum calcium is a useful marker for the difference in calcium homeostasis.[19] In this same study, it was found that calcium levels are positively associated with breast cancer in overweight peri-/post menopausal women unlike women in their premenopause.[19] As a result of the hormonal change that occur, the misregulation of calcium level in breast tissue typically seen after menopause is suspected to result in calcification.

Calcifications are results of small calcium deposits that develop in the breast tissue, which commonly happens after menopause due to hormonal changes with an increase in age.[19] The calcification clusters are not necessarily related to the calcium from our diets either. Calcifications have been proposed to be the result of the deposition of calcium oxalate and/or calcium phosphate in the breast; however, the mechanism of the deposition is not clearly understood yet.[20] Calcium oxalate is produced by apocrine cells in the breast and is mainly related to benign cystic change. Excess exposure to calcium oxalate could affect the epithelial cells by triggering cellular and genetic changes, which promotes the transformation of breast cells from normal to tumor cells.[20,21] Although the exact mechanism of calcification is not known, there are two scientific hypotheses: 1) calcium secretion by glandular cells and 2) inability to clear regions during cell death. Sometimes the granular cells of the breast can also release calcium into ducts, as the primary job of

cells in that area is the secretion of milk. These calcifications then appear in the ducal system, the breast acini, stroma, and vessels, mainly as calcium oxalate and calcium phosphate. The second scientific hypothesis states the potential for the formation of calcification from the deposition of dead cells in the breast tissue microenvironment. The growth of unchecked cells crowding an area causes cell death but, if the body does not flush dead cells out, they accumulate with a potential to form calcium deposits.[22] Calcifications formed this way harden the breast tissue by converting into carbonates or some other insoluble calcium components. In most instances, these calcifications are benign (noncancerous), but certain types of calcification clusters could be indicators of underlying breast cancer development. These two hypotheses do not necessarily work synergistically instead it is either one or the other hypothesis that promotes the growth of tumor cells. However, regardless of the mechanism of calcification clusters formation in breast tissue, we need to have a technique to identify and ideally differentiate the types of calcifications based on the type of calcium deposits (mainly tiny calcium deposits).

There are various patterns of calcification that occur in the breast which helps in differentiating benign and malignant conditions. Calcifications could be larger or smaller in size, therefore, a knowledge of calcification patterns during breast image analysis is critical to distinguish benign from malignant. One way to differentiate calcifications is to assess their morphology, size, appearance, and distribution in the breast. There are two types of calcifications in breast tissue: microcalcification (MCs) and macrocalcification. Macrocalcifications are defined as large typically >2 mm calcium deposits in the breast tissue that are typically associated with benign, such as fat necrosis.[20] They have a defined shape (i.e Euclidean objects) that is mostly distributed or scattered randomly in a large

volume (>2 cm^3) throughout the breast microenvironment which often involves most of the area in the breast. Macrocalcifications are large and mostly well-defined calcifications that often appear as a line or as a dot in the mammogram. The different patterns of macrocalcifications are seen and/or associated with the different parts of the breast. For example, thin, round, and rim-like shape (Figure 2A) are often seen in the walls of cysts (fat necrosis), coarse and popcorn-like shapes (Figure 2B) are often seen in degenerative fibroadenomas, singe or parallel linear railroad patterns (Figure 2C**)** are often referred to as vascular calcification, large and rod-like deposits (Figure 2D**)** often follow the ducts toward the nipple, small rounded soft-tissue shadow looking (Figure 2E**)** often are milk calcium, and round lucent-centered deposits (Figure 2F**)** often represent dermal calcification.[23]

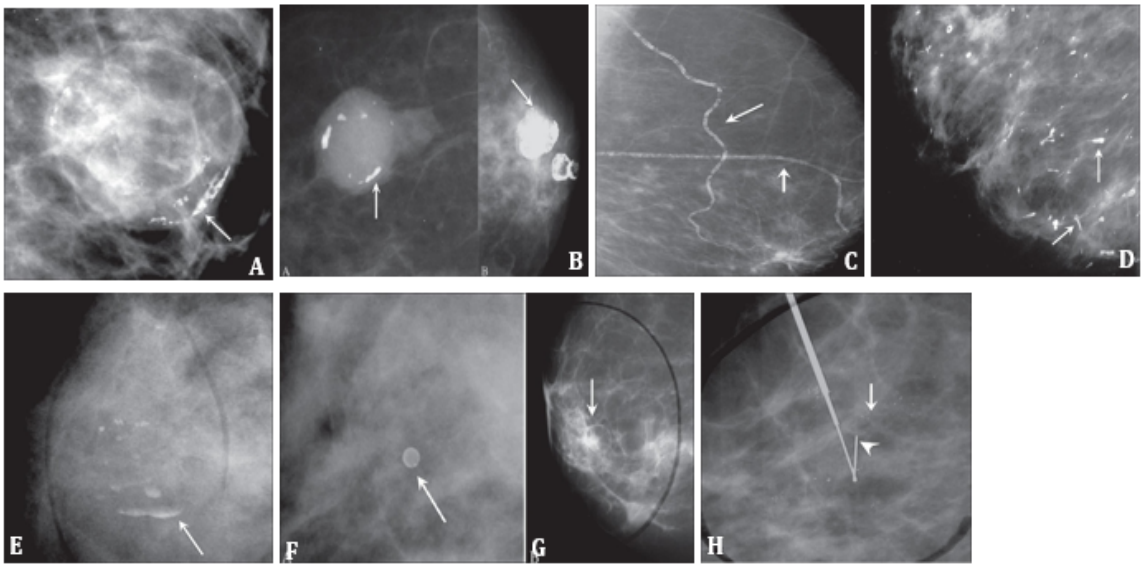

Figure 2: Macrocalcifications detected in a mammogram. **A**. rim or egg-shell type calcification. **B**. degenerating fibroadenomas with coarse (A) and popcorn (B) calcification **C**. linear, railroad track vascular calcification. **D**. thick, large, rod-like calcific foci. **E**. soft-tissue shadow of calcium with layering. **F**. a lucent-centered focus of dermal calcification. **G** large, lucent-centered oil cyst. **H.** Intermediate concern amorphous calcification clusters. Adopted from Ref. [20]

On the other hand MCs are defined as smaller typically < 0.5 mm calcium deposits in the breast tissue associated with malignancy such as ductal carcinoma in situ or invasive carcinoma.[23] The same study that was conducted to evaluate calcifications indicated that patterns with fine, linear, segmental, branching or casting (Figure 3A**)** and pleomorphic calcifications (Figure 3B**)** (calcifications of varying shapes and size) are often associated with microcalcifications.[23] This project is based on the analysis of MC clusters in mammograms to differentiate them us benign and malignant clusters.

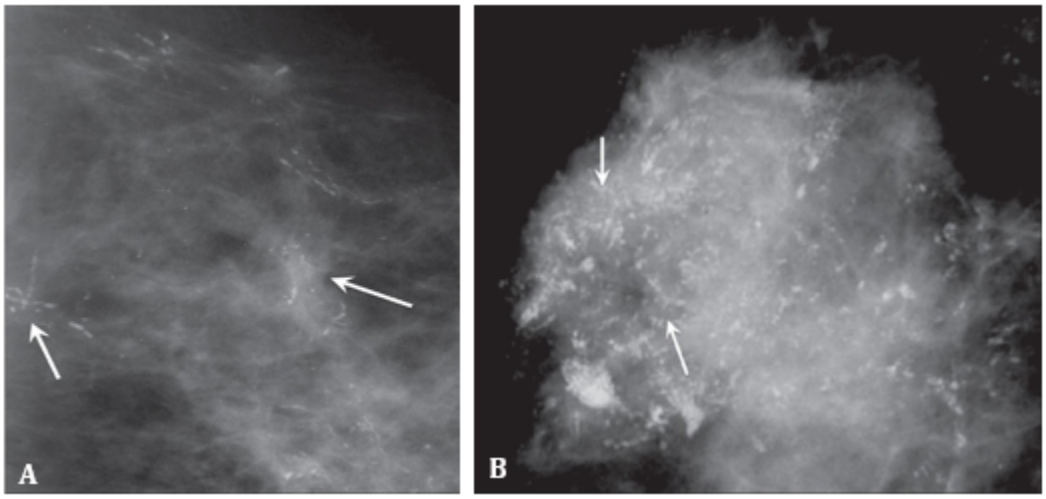

Figure 3: Microcalcifications typically associated with malignancy shown in mammograms. **A.** fine, linear, branching calcifications. **B.** pleomorphic calcifications (ductal carcinoma).
Adopted from Ref. [20]

The appearance and or the distribution of these two different calcification clusters in mammography is one way to explain the state of the breast. If the calcifications are grouped or clustered loosely (i.e <10/cm^2) they are associated with a benign condition but, if the calcifications are clustered in compact cluster (i.e >20/cm^2) they are associated with a malignant condition.[24] A research that studied the average size of MC clusters in an area in order to differentiate clustering of MC in mammograms for benign and malignant cases

found that the mean number of microcalcifications per 0.25 cm^2 was 16.4 in malignant and 16.7 in benign.[24] The result from this study showed no statistical significance to differentiate MC clusters in benign and malignant cases by looking at their average size per a defined area in mammograms. Although the above and other studies in breast cancer calcification differentiation have revealed the distribution, clustering, and pattern of calcification clusters, microcalcification identification in breast image analysis could be easy to miss. Additional factors that make the interpretation challenging is that some deodorant or lotions applied on the skin appear in patterns that mimic calcification clusters when images through mammography.

Radiographic microcalcification was first described in 1913 by Albert Salmon, a surgeon in Berlin, who imaged over 3,000 surgical specimens describing the association of microcalcifications with breast cancer and specimens that demonstrated tumors spreading to the lymph nodes.[2] To conclude this introductory exposition about microcalcifications, MCs are smaller in size (compared to macrocalcifications) and oftentimes they appear as clusters or randomly dispersed in the breast tissue. The detection and classification of calcification clusters (in particular MCs) in a breast image is very important for early detection of breast cancer. The early detection of cancer is very important to provide patients with the necessary therapies or other treatments, or advice in maintaining dietary health. In general, the development of a computational model that adds assistantship for the radiological interpretation of breast images will help in minimizing the number of women who suffer from treatments e.g, chemotherapy and save those who would have died of the disease.

CHAPTER 3: EPIDEMIOLOGY

Breast cancer is a very common worldwide disease affecting the lives of many women with an increasing rate worldwide. It is the most frequent cancer among women and holds the second places in cancer related death. A report by the World health organization showed that about 2.1 million women get infected each year.[25] About 1.67 million new cases were diagnosed in 2012 and in 2018 the estimated number of women died from breast cancer is about 627,000.[25,26] According to the World Bank classification strategy, there are three major categories in health care investment, based on the gross national income of the country. These three major categories are: Low Income Countries (LICs), Low Middle Income Countries (LMICs), and High Income Countries (HICs). LICs and LMICs are mostly classified as developing countries, and countries with HICs are classified as developed countries. When looking at a country's annual income level, the terminologies "developing" and "developed" are not necessarily used to define the development status of a country; rather, they refer to the ability of the country to provide adequate health care. In addition, this classification provides insight to how much the country invests in providing the most relevant health care. Health care in developing countries to provide breast screening for an early stage cancer detection might not be easily accessible, unlike in developed countries. Because of the inability to provide reliable breast screening, along with many other difficulties in getting the proper treatments, breast cancer has a higher mortality rate in developing countries when compared with developed countries. This is despite the fact that people in developed countries are affected at a higher rate than developing countries. Breast cancer leads to approximately 500,000 cancer deaths among women annually.[26] The highest incidents occur in the most developed regions of

the world, with 74.1 new cases per 100,000 women, in comparison to the 1.3 new cases per 100,000 observed in less-developed regions.[26]

Data collection in developing countries is very challenging, as it is extremely scarce; however, studies have shown that the survival rate for cancer in developing countries (LICs and MLICs) is lower than developed countries (HICs). Observing a 5-year survival rate in female populations, a study found that in HICs countries like China, Singapore, South Korea, and Turkey the median relative survival rate of breast cancer were 76-82%, whereas in LCIs countries like Gambia, the survival rate was 22%, and Uganda was 46%.[26,27] These survival rate values indicate the level of development in the health care of the country to provide the necessary early diagnosis, treatment, and follow-up clinicals for all patients. In developed countries there is better health care service and there are many accessible advanced technologies that are used to treat patients with a relatively affordable price. However, in developing countries the level of development of the health care is relatively low with a very limited access to advanced medical technology for early diagnosis, treatment, and clinical follow-ups. In addition, people who live in developing countries have lower income with little to no affordable life insurance to help cover the price of health care costs.

3.1 Breast Cancer in Developing Countries

Breast cancer has a higher effect on families in developing countries than in developed countries in every aspect. Women in developing countries have more responsibilities in their family setting and within the society than women in developed countries. Any consequences that come with breast cancer like financial burden and the need for time to take care of themselves are real challenges that these women face as they

work restlessly to fulfil their responsibility. In addition, most of these women do not have as much access to advanced health care services for early diagnosis of breast cancer. Breast cancer is a rising world problem mostly in developing countries with studies as of 2002 showing it holds the fourth place in its effect on both sexes (men and women). Due to this huge health care problem in developing countries, the disease is more aggressive in killing many women which increases the mortality rate of that country per year. The shortage in availability of health insurance companies to help cover the cost needed to get the diagnosis and treatment of breast cancer is one other factor for the rise in death rate from breast cancer. Most of the time health care providers like big hospitals are found in urban areas rather than the rural areas and so women who live in the countryside do not have as much opportunity to visit specialized doctors. Along with this, the literacy rate of women in the countryside is lower than women in the urban areas which makes a difference in the understanding of the effect of breast cancer and the initiation to seek help. Women in underprivileged areas of Africa and Asian countries are unaware of the importance of breast cancer screening and the necessary treatments needed after the diagnosis. All of these predominant risk factors increase the number of women being affected by the disease increasing the mortality rate which also affects the economy of the country.

A study conducted in North-Africa has shown that breast cancer is the most common cancer among women representing 25% to 35% of cancer types that affect female.[28] The major risk factors in these areas include: family history, age at menopause, age at menarche, breastfeeding, number of children, age at first child, oral contraceptives, hormone replacement therapy, alcohol, and body mass index.[29] Patients with a family background of breast and/or ovarian cancer have a risk of getting breast cancer either from

first, second, or third-degree relatives. In this same study, it was reported that approximately among the 30% of patients that were diagnosed for breast cancer, it was found that 7-9% of them had breast cancer in their family history.[29] Menopause is defined as the cessation of menses and the termination of ovarian follicular maturation due to loss of the ability of the ovary to produce estrogen in significant quantities. The hormonal changes during this period in some women could be a cause for health consequences like breast cancer. Some of the reasons include: the increase in calcium retention in the kidney, calcium reabsorption from the skeleton, and calcium reabsorption from the intestine before and after menopause. The mean duration of breastfeeding time is significantly associated with a reduced risk of breast cancer. Women whose lifetime breastfeeding duration is more than 73 month has a lower risk of breast cancer.[29] Studies have also shown that a longer duration of breastfeeding time along with menopause status reduces the risk factor of breast cancer. Overall, this analysis done on women in North African countries indicate breastfeeding reduces the incidence of breast cancer by 4.3% for every 12 months and incidence increase by 3% for every year menopause is delayed. Other risk factors that are associated with breast cancer incidence include 16% reduced risk for every two births, 40% increment for first birth after age 35 versus age before 20, 7% reduction for each year menarche is delayed, and 32% increment for an intake of 35-44 g alcohol/day.[29–31] Even though these statistical values represent North African women, these risk factors are common problems of most developing countries, especially in African countries.

Women in developing countries do not visit a doctor on a regular basis unlike most females in developed countries. The main reasons for this are the limited access to hospitals to go for screening and the available doctors to diagnose patients. Most of the time patients

also do not visit doctors until cancer reaches the latest stage; even if the patient gets the opportunity for early cancer stage breast screening, the patients do not seek treatment. This delay in diagnosis facilitates the progress of the disease and the delay of getting the necessary treatment minimizes the chance of survival. Due to this reason in many developing countries, breast cancer is a slowly rising disease with high case-fatality rates leading to the death of many adult women. This high case fatality rate is approximated by the ratio of the mortality to the income across the developing world which further reflects the inequities in early detection and access to treatment.[32] According to the most recent Globocan/IARC data the number of deaths as a percentage of incidence cases in 2008 was 48% in LICs and 40% in LMICs.[33]

Digital mammography and other advanced technologies for breast cancer diagnosis are complicated and expensive resources. Screening and treatments are not readily available for all women, therefore, the easiest way to address the problem is by creating awareness. Educating women to live a healthy life, minimizing alcohol, exercising, maintaining a healthy ideal body weight, and avoidance of postmenopausal hormone replacement therapy can have a significant impact in reducing the probability of getting breast cancer. According to World Health Organization, implementing these knowledge into action could prevent up to one-third of new cancers and survival for another one-third of cancers detected at an early stage.[34] However, in addition to all these precautions to prevent breast cancer and while many of the developing countries still battle for advanced medical technology there is a high need for affordable and accessible healthcare for early physical examination. The combination of education and effective healthcare service by

trained medical personnel with the assistance of easily applicable technology has the potential to enhance the fight against breast cancer.

3.2 Breast Cancer in Developed Countries

Breast cancer in HICs, developed countries, is much more controlled than in LICs and LMICs, developing countries. Majority of the women in developed countries have easy access to using adequate healthcare for an early breast cancer diagnosis and getting the necessary treatment to prevent the cancer from growing to an advanced stage. In HICs one of the greatest options that are readily available for women both in urban and rural areas is the presence of health insurance companies that can assist individuals and families financially. In addition, women in these countries are also educated better than women in developing countries which plays a huge role in fighting against the disease.

Digital mammography screening in developed countries is the most common way for early detection of breast cancer and it is highly associated with the reduced mortality rate of cancer in developed nations. According to the International Agency for Research on Cancer (IARC), there is sufficient evidence to show the reduction in the effective rate of breast cancer among screened women of age between 50-74.[35,36] Women in this age range have indicated that the mammographic screening has reduced their risk of dying from breast cancer by 23%. In general, those women who attended the screening program that IARC has organized for this case-controlled study had about 40% reduction in the risk of breast cancer.[36] However, one of the problems with that could be associated with mammographic screening for early breast cancer detection is the high probability for false diagnosis resulting from potential misinterpretation of breast mammograms.

CHAPTER 4: EXISTING SOLUTIONS

Cancer has been in medical history since as early as 1600 BC in the Edwin Smith papyrus, where the oldest description of the illness existed.[37] In the 2nd century AD, Aleius Galenus (mostly referred as Galen), an ancient Greek physician and surgeon, made a detailed categorization of abnormal growths (tumors), which he had seen occurring more often in the breasts of women whose menstruation was either abnormal or inexistent.[37] However, he had also suggested that cancer would better be treated at its early stage, otherwise surgery would be a better solution for late stage cancer. Leonides of Alexandria near the 2nd century AD distinguished between the scirrhous (a hard cancerous growth usually arising from connective tissue) and cancer in the breast, suggested the amputation of the breast for any late stage cancer.[37] Both of these two ancient physicians and other ancient physicians, as well as modern doctors, explained that surgical treatments for cancer past the early stage is an effective way of treating the disease.

4.1 Modern Breast Cancer Diagnosis

The most common technique that is being used to diagnose breast cancer in modern times is breast screening. In 1975, about 45 years ago, a controlled trial of about 31,000 women age 40-64 were selected for a population study to determine the effectiveness of breast cancer screening with mammography and clinical examination.[38] Results from this study showed that screening had led to a 30% reduction in cancer mortality rate.[38] Since 1977, breast screenings for women above age 40 has been recommended for early detection of cancer. However, guidelines for a proper screening were not yet well established until 1997. Then in 2002, the United States Preventive Service Task Force recommended

screening mammograms every two years then in 2016 they recommended getting breast cancer screening every year for women of age between 50-74.[39]

4.1.1 Current Imaging Techniques

The use of screening techniques to diagnose abnormalities in breast cancer has evolved rapidly in the 20th century with mammography having been fully developed in the 1960s.[40] The history of mammography is divided into three phases; the foundation of mammography was laid in 1913 by the observation that a German surgeon made, from 1940 - 1970 followed the development of mammography by different radiologists and industry, and the last phase started close to the end of the 20th century where breast cancer screening started.[38] At the last quarter of the 20th century, most of the modern techniques like ultrasound, magnetic resonance imaging (MRI), and digital mammography started to be used for breast cancer screening.[41] The third phase of the development is when most women started to be screened for breast cancer. The quality of mammography has improved since 1950_s where Greshon Cohen and his associates have identified benign and malignant abnormalities, and further reported on the potential of mammography as diagnosing tool.[42] A report posted in 1973 on the results of the Health Insurance Plan of Greater New York randomized, controlled, breast cancer screening study showed that women who got breast screening 5 years before the report was made has showed a one third reduction in breast cancer mortality rate.[42] In the late 70s, sonography, a medical diagnostic method using high-frequency sound waves like ultrasound to create an image of the breast, was developed, which complemented mammography.[41,43] Nevertheless, this technique was not efficient enough to replace mammography fully as it lacks the ability to detect the presence of microcalcifications, which are a major indicator for the formation of

breast cancer. By the end of the 80s, MRI became a more important diagnostic tool, but it was not efficient enough to detect the presence of microcalcifications and it was too expensive to be used by every health care center.[43] Even though mammography has been recognized as a medical diagnostic technique for breast cancer screening, there is still a need to improve the CAD system to improve mammogram analysis for a better patient care.

Mammography. There are two different kinds of mammography: digital mammography and film mammography. Digital mammography refers to the application of digital system, techniques, on mammography, which are created when a conventional mammography is digitized to be used in computers.[44] Film mammography refers to a system where breast images taken using conventional mammography are read and stored on film. The use of conventional breast screenings by radiologists has created problems of increased probability of false diagnoses or negative readings, which decrease the chance for early detection of abnormalities in breast tissue.[41] As a greater density of breast tissue reduces the sensitivity of mammography, digital mammography is made to improve film mammography, as it separates and optimizes image acquisition and display.[41] According to a research study that was conducted to test which of the two mammography techniques would better analyze breast cancer in young women, premenopausal and perimenopausal women, and women with dense breasts, it was understood that digital mammography is more efficient than film mammography.[41] There is no significant difference between these two techniques, however, digital mammography offers easy access to images, can easily work with CAD, and uses a lower average dose of radiation without a compromise in diagnostic accuracy. In digital mammography, X-ray transmission could be manipulated

to adjust image contrast, which enhances the visualization of problematic areas (areas where mass or clusters of calcifications are present) like adjacent dense tissue where the cancer tumor could probably hide without altering its accuracy in diagnosis.[41]

Mammographic images are taken from different angles, but the major views that radiologists look into are the cranial-caudal (CC view) and mediolateral oblique (MLO). In the CC view, the entire breast is depicted as the breast is flattened out in between two plates at exactly 180^{o} and/or 0^{o}, whereas in the MLO view, the breast image is taken from a 90^{o} projection as shown in Figure 4.[45] Both of these views together must show the medial part as well as the external lateral portion of the breast. The CC projection may show the pectoral muscle on the posterior edge of the breast, indicating that the breast is positioned as forward as it could go.[46] The MLO projection is a very important view as more of the breast tissue are captured in the image and the lateral side of the breast is predicted to be the most common place for pathological changes.[46] In MLO view, the amount of pectoral muscle that is showing in mammograms is an indicator for the amount of breast tissue that is included in the image.

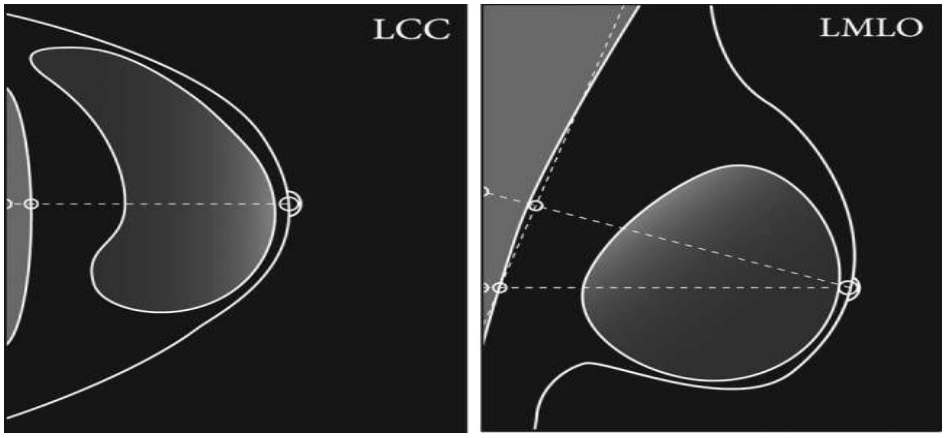

Figure 4: The CC (180^{o} and/or 0^{o} projection) and MLO (90^{o} projection) views of mammographic breast image. Adopted from Ref.[45]

Magnetic Resonance Imaging (MRI). Breast magnetic resonance imaging (MRI) has a very high sensitivity degree in detecting breast cancer, regardless of the breast tissue. MRI is very useful, especially for those women who are at a higher risk of getting breast cancer, which includes women with genetic predisposition and women with a family history of ovarian and/or breast cancer.[47] Breast MRI has the potential to detect abnormalities in breast tissue better than physical examination, mammography and ultrasound. But MRI is not effective in identifying microcalcifications inside the breast tissue. MRI is effective in identifying some occult tumors in a very dense breast tissue, for which mammography usually has difficulty in identifying the size and shape of abnormal spots.[48]

The use of MRI has shown a greater impact on the diagnosis of breast cancer, however, distinguishing fat from a critical tissue lesion is a challenge in breast MRI. In a study that was held to assess the effectiveness of MRI, it was found that breast MRI has identified suspicious lesions in 76% of stage II patients and 86% of stage IV patients.[48] As tissue lesions could be a potential area for malignant cancer growth, it is very important that they are identified and distinguished in any breast image. One of the challenges in breast MRI is that there are a group of women in a small percentage whose normal glandular tissue exhibits intermediate to strong early phase enhancement after contrast administration, which could result in false positive diagnosis.[47] Nevertheless, breast MRI cannot be used as the only means to diagnose breast cancer for early stage detection. Rather, it is more effective when it is used in alternation with mammography.

4.2 Challenges with Existing Solutions

Breast cancer is easily detected using different imaging techniques in which the presence of irregularly or abnormally shaped structures are detected to characterize and discriminate between cancerous and non-cancerous tissue. Despite its usefulness, medical imaging is a challenging task and it requires input from different trained people and digital aid from technologies. Digital mammography has been in application for a long period of time, helping to minimize the breast cancer mortality rate. Since CAD techniques have been introduced to the medical field, particularly to digital mammograms, they have assisted radiologists by providing a useful computerized vision. However, CAD usage has been associated with increased false diagnostics and unnecessary biopsies, which lead to stress to the patient and a financial burden to the healthcare system.[49–56]

CHAPTER 5: APPLICATION OF FRACTAL GEOMETRY IN BREAST CANCER DIAGNOSIS

Fractal geometry studies non-Euclidean objects or objects with an irregular shape whose dimensions are statistical quantities indicating how irregular the object is rather than a commonly defined integer dimension. Fractals by nature repeat themselves as the bigger object is zoomed into finer pieces, exhibiting details at every size scale. These objects exist in nature, biology, medicine, and everywhere. Euclidean geometry is used to describe objects that have a smooth shape: lines, circles, cubes, etc. However, fractals do not possess the characteristics of the so-called Euclidean geometry. One of the major differences that B. Mandelbort (father of fractal geometry) has identified when he first introduced fractal geometry is self-similarity. One of the simplest objects to illustrate this concept of self-similarity in fractals is Sierpinski's triangle (Figure 5). All the smaller triangle pieces are similar to the full-size set. In nature, however, such self-similarity is not exact like Sierpinski's triangle, but rather, the self-similarity is statistical.

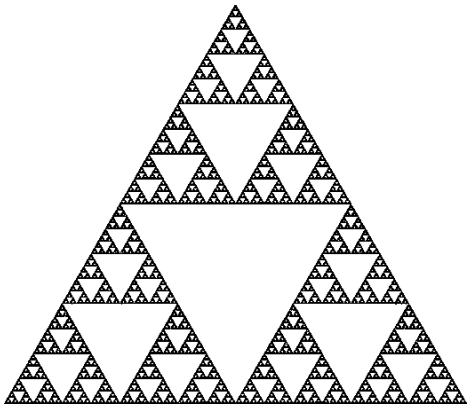

Figure 5: Sierpinski's triangle

The fractal dimension is a tool used to describe fractal objects quantitatively in order to characterize how much space they occupy. The non-integer fractal dimension of fractals sits in between the Euclidean, integer dimensions. One way to estimate the fractal dimension for 2D objects is by using the box counting method. This method accounts for the power-law relation between the number of boxes of various sizes that are required to cover the fractal set and the radius of each box to calculate the fractal dimension:

$$D = \log N(r) / \log (1/r) \qquad \text{Eq. 1}$$

where N(r) is the number of boxes of radius r needed to cover the space, and D is the fractal dimension obtained from the slope of the log-log plot of N and $1/r$. However, the box-counting method is not easily applicable in image analysis. For example, an image of the breast taken by digital mammography may have a multifractal nature but since the box counting method is limited in its applications it cannot be used to study the fractality of breast tumor. Therefore, a more powerful method is a requirement to improve early cancer detection. In this project the fractal dimension of breast tumors (MC clusters) calculated from the analysis of mammograms with the aid of the 2D WTMM (further discussed in section 5.1) is explored.

Another area where the analysis of images with multifractal nature plays part is in its use to study the architecture of breast microenvironment surrounding tumors. As described in Chapter 2, MC clusters have different forms of morphology and irregularity in their architecture inside the breast tissue which radiologists have mostly been using qualitative ways of describing malignancy and tissue lesion. Previous researchers have studied the use of fractal characteristics in ultrasound images to analyze microcalcifications

and differentiate tissue lesions to distinguish benign from malignant.[44] The most frequently used technique in analyzing digital mammography images using fractals is to use a fractal-based segmentation technique to analyze the self-similar nature in microcalcification clusters.[47] This way of analyzing mammograms provides a better insight to tissue architecture and disruption with the ability to quantitatively assess tumor cell growth. In general, the use of techniques like this for the analysis of complex images like mammograms has shown a promising methodology in understanding the state of tissue homeostasis of the microenvironment surrounding the MC clusters.

One way to analyze mammograms to investigate the microenvironment surrounding tumors is to study image density fluctuations, i.e. surface roughness, as quantified by an exponent such as the Hurst exponent. Several techniques can be used to estimate such roughness exponents, including the autocorrelation function, the root-mean-square analysis, the Fourier power spectral analysis, and the 2D WTMM method (for example, see Ref [57]). Even though the H values that are used later in this thesis were obtained from the 2D WTMM method, for simplicity, a brief overview of the Fourier power spectral analysis follows.

A Fourier power spectral analysis consists in studying the power-law relationship between the Fourier spectral power vs. spatial frequency. In statistics, the power-law states that a relative change in one quantity results in a proportional relative change in another. Fractal functions are functions that show the representation of multiple frequencies at play where there is not necessarily one dominating frequency (represented as one peak in the power distribution), but rather, a power-law distribution of spectral power spectrum vs. the spatial frequencies. These functions behave like a power-law.

$$S(k) \sim (1/k)^{\beta} \qquad \text{Eq. 2}$$

where $S(k)$ is the power spectrum, k represents the spatial frequency, and β is the power spectral exponent, which is related to the Hurst exponent, H, quantifying roughness.

$$\beta = 2H - 2 \qquad \text{Eq. 3}$$

As mentioned above, this concept of quantifying roughness using the Hurst exponent has been applied in different studies, the Hurst exponent values used for this project are not obtained by the power spectral analysis instead they are results from the 2D WTMM analysis method.[7]

5.1 The 2D Wavelet Transform Modulus Maxima Method

The Wavelet Transform Modulus Maxima (WTMM) method is a multifractal formalism used to analyze complex 1D signals, 2D images, 3D images, and vector fields.[58] Wavelets are rapidly oscillating signals that are useful in analyzing the singularity of fractals and the WTMM can be used to estimate the strength of these singularities in a signal. Singularity in mathematics refers to the non-defined shape or irregular regions of an image that lacks differentiability or analyzability as compared to defined shapes. Therefore, the WTMM method is a way of performing multifractal analysis in a multifractal formalism using wavelets instead of boxes. The WTMM were first explored by Mallat and Hwang in 1992 for signal processing purposes to compute the singularities of 1D functions.[59] Then A. Arneodo developed the WTMM method as a multifractal method, first in 1D,[58,60] and then in 2D, 3D, and for vector fields.[61,62]

The wavelet transform (WT) is a mathematical microscope that is capable of analyzing complex non-stationary time series.[61,62] The continuous WT characterizes spatial image information over a continuous range of size scales. The increase in magnification in this singularity scanner can reveal and quantify details of a signal irregularity using the Holder exponent, h.[63] A previous study conducted in 2014 by CompuMAINE lab has shown that the 2D WTMM method is promising to be used in studying the architecture of breast tissue lesion. In the study, multifractal analysis of mammograms was performed, where the Holder exponent, *h,* characterizing the strength of singularity was used to differentiate the MC from the background tissue. MCs were segregated from the background tissue by considering two pieces of information: the strength of the modulus of the WT at the smallest scale and the variation of the slope, *h,* across the scales.

The breast in Figure 6 shows the 2D WTMM analysis of a dense tissue whose roughness fluctuation is characterized by a relatively high smoothness level. The image in Figure 6A and 6B show the mammogram of a dense breast and suspicious region containing MC clusters circled by a radiologist respectively. The images from Figure 6C to 6G shows the 2D WTMM analysis of the circled region segmenting the MC (red) from the background tissue (blue). After the segmentation was done, the fractal dimension, D, of the lesion was calculated. As the histograms in Figure 7 demonstrate, the outcome of this study reveals that benign lesions have fractal dimensions with a strong preference for Euclidean dimensions, either to the far right (=2) or to the far left (=1), whereas malignant lesions have fractal dimension with a strong preference for the middle of the curve with a value between $1<D<2$.

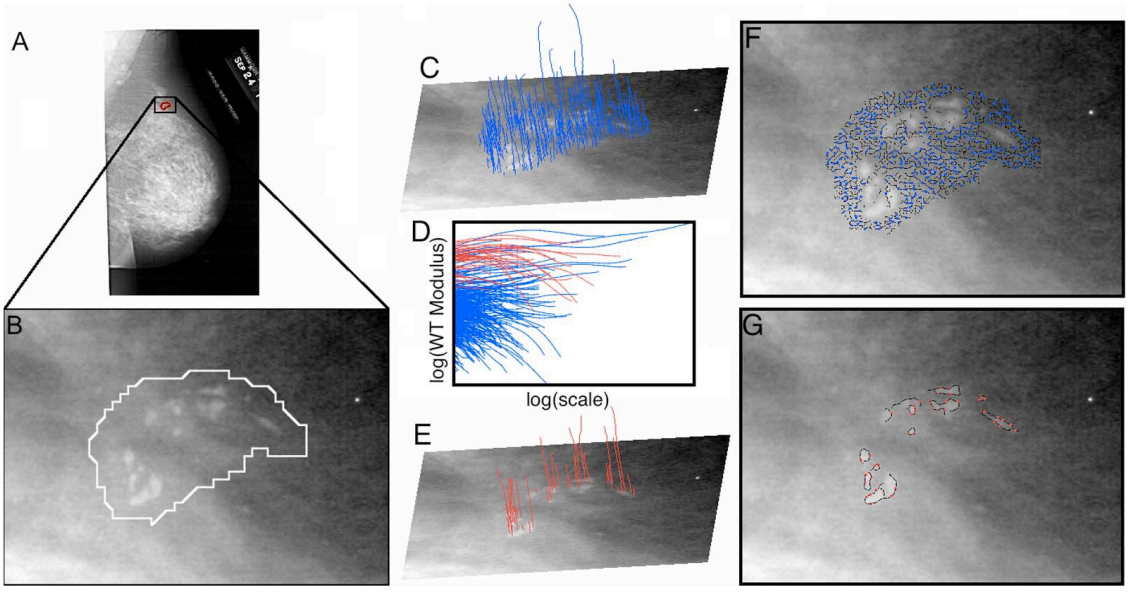

Figure 6: Sample 2D WTMM analysis of a malignant breast lesion. **A**. mammogram of a dense breast tissue. **B**. suspected area of microcalcifications circled by a radiologist. **C-G** the 2D WTMM analysis of the circled region to differentiate between MC clusters (red) and the background tissue (blue) surrounding them. Adopted from Ref.[7]

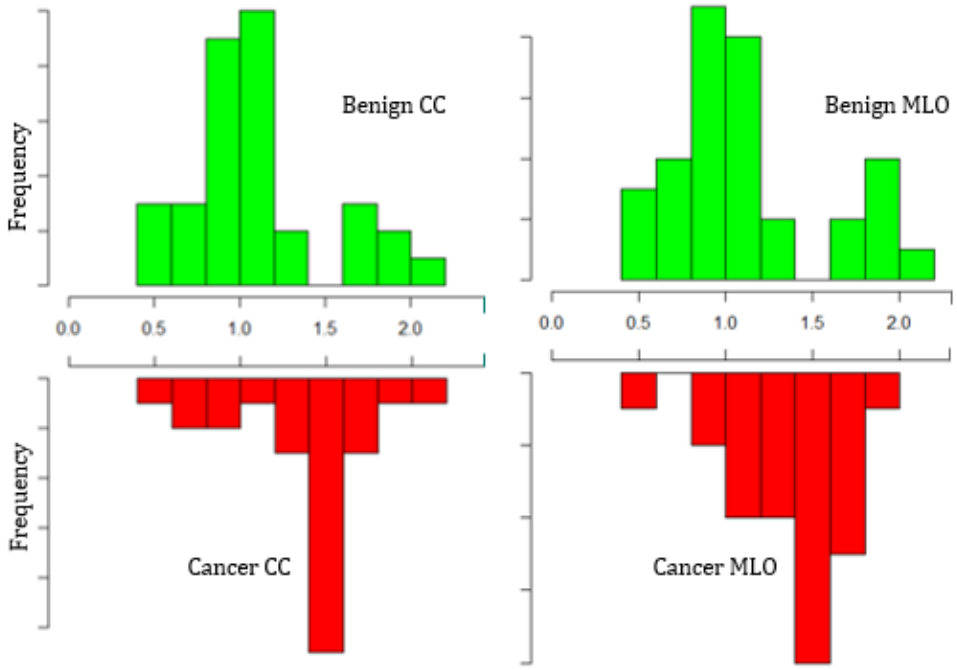

Figure 7: Histogram plot of the fractal dimension, *D* for both benign and malignant in both mammographic views. Adopted from Ref. [7]

The histograms in Figure 7 indicate the preference in (non-integer) fractal dimension for malignant vs. Euclidean dimension for benign in both CC and MLO views separately. The 2D CC-MLO fractal dimension plot in Figure 8 is an additional evidence that shows the difference between malignant and benign cases. In this plot the x-axis corresponds to the fractal dimension values for both benign (green) and malignant (red) MC clusters from the CC view and the y-axis corresponds to the fractal dimension values for both benign and malignant MC clusters from the MLO view. The identified polygonal region in Figure 8 shows that benign cases prefer the region outside the polygon which is identified to be the Euclidean zone and the malignant cases prefer the region inside the polygon which is identified to be the fractal zone.[7]

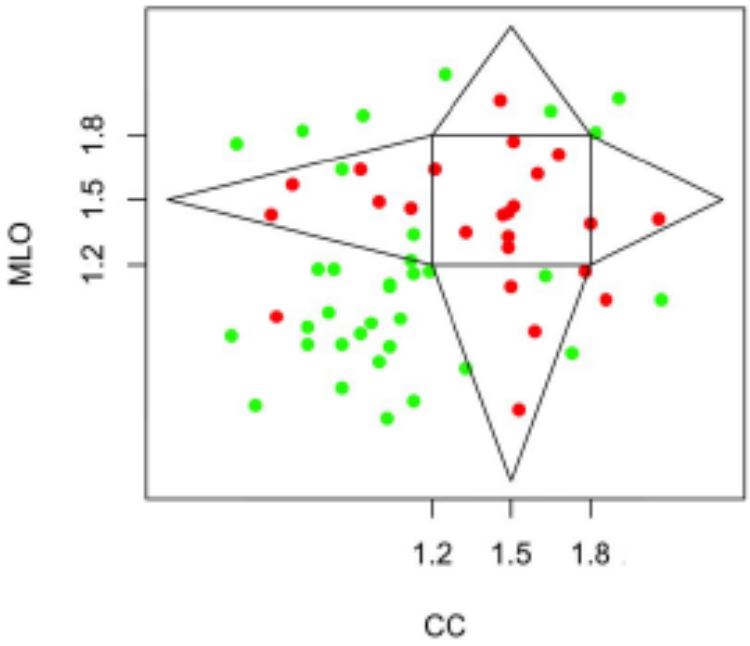

Figure 8: The CC-MLO fractal dimension plot is a graph of all the benign and malignant cases fractal dimensions from the MLO view as a function of fractal dimension from the CC view. The red dots represent malignant cases and green dots represent benign cases. Inside of the polygon is defined as the fractal zone and outside of the polygon is defined as the Euclidean zone. Adopted from Ref. [7]

This same research team conducted another research in 2017 using the 2D WTMM method aiming to show that tissue disruption and loss of homeostasis in breast tissue microenvironment, and breast bilateral asymmetry can be quantitatively and objectively characterized by assessing mammograms. The density fluctuation in the microenvironment of the breast due to tissue disruption was quantified by using the Hurst exponent, *H*. The Hurst exponent, *H* is a quantifier of the global roughness of an image density fluctuation which was first introduced to the 2D WTMM analysis of mammogram by Kestener et al.[64] This is a potential tool to discriminate dense and fatty breast tissue as dense tissues are mostly described as risk areas of breast cancer. The density fluctuations in healthy breast tissue are either monofractal anti-correlated with $H<½$ for fatty tissue or monofractal long-range correlated with $H>½$ for dense tissue.

The outcome of Kestener's study has shown that fatty areas have *H* - 0.30 whereas dense areas have *H* values ~0.65. But although promising, Kestener's study was based only on a handful of mammograms. In a seminal paper published in 2017, the CompuMAINE Lab improved the approach, scaled it up to hundreds of mammograms, and made an important discovery, which has led to the recent award of a patent.[65] After the calculation of *H* values was done a sliding window technique using the 2D WTMM method was used to determine the parameters that are most effective in distinguishing between normal and tumorous cases. The results demonstrated that disrupted regions associated with loss of tissue homeostasis are quantified by $H\sim½$.[11] The values for *H* were associated with colors, as shown in Figure 9 yellow for $0.45<H<0.55$ (disrupted tissue region), blue for $H<= 0.45$ (fatty tissue) and red for $H>=0.55$ (dense tissue).[13] In general, in this study the team was able to develop the "yellow square analysis" based on *H* signature for different regions in

the breast microenvironment which has moved the process of studying the correlation between tissue disruption with loss of tissue homeostasis one step forward.

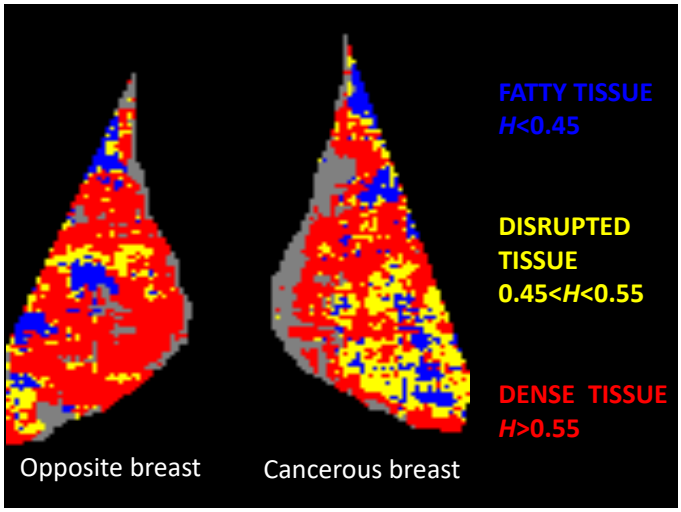

Figure 9: Sliding-window analysis of a cancer case showing more disrupted (yellow) tissue in the cancerous breast than the opposite breast. Each pixel represents a 360 x 360-pixel mammogram sub-region colored according to its *H* value. Taken from Ref. [11]

5.2 Analysis and Discussion

This project consists in revisiting existing data from the CompuMAINE Lab, where a wavelet-based technique was developed and launched on a dataset of mammograms with MC clusters. The mammograms for data analysis were taken from an online data bank called the Digital Database for Screening Mammography (DDSM). They are the same sets of mammograms that were used in the CompuMAINE Lab's 2014 study.[7] The obtained mammograms included both the MLO and the CC view of 33 benign cases and 25 malignant cases. The images were analyzed using the 2D WTMM method where the fractal dimension for the MC were already calculated and published in 2014. Also calculated at the time, but not included in the 2014 paper were the Hurst exponents for the background microenvironment tissue surrounding the MC's (based on the blue curves shown in Figure

6 C, D, and F)[7]. For this project the values for the fractal dimension were collected in order to study its correlation with Hurst exponent, *H.*

The values for both fractal dimension, *D,* for the MC clusters and Hurst exponent, *H,* for the background tissue were obtained from the 2014 study's results spreadsheet for further analysis. A separate excel spreadsheet was prepared with columns containing just values of *D* and *H*, for both MLO and CC views. We then graphed the fractal dimension, *D*, as a function of the Hurst exponent, *H*. R[66] was used to plot two separate "2D Hurst exponent vs fractal dimension" graphs for CC and MLO views, as shown in Figures 10a and 10b, respectively. The behavior of the data points for both benign and malignant cases was then studied to identify a region that best represents the relationship between the Hurst exponent and the fractal dimension in distinguishing between the two cases (benign and malignant) in both CC and MLO view. From this plot the quadrilateral region is identified as a region of interest to show the difference between benign and malignant cases. The quadrilateral region extends in the x-direction from Hurst value of 0.2 to 0.8 centered at 0.5 and it stretches vertically from fractal dimension value of 1.0 to 2.0 centered at 1.5. The range for *D* value from 1.0 to 2.0 was selected considering that MC clusters have a fractal dimension in between Euclidean dimension as shown in the histograms in Figure 7. The Hurst exponent range from 0.2 to 0.8 was chosen considering that disrupted tissue regions have Hurst between $0.45<H<0.55$ and to further encompass both fatty and disrupted tissue regions according to Figure 9. Based on a manual count 15 malignant cases out of 25 cases (60% of all the cases) in CC view (Figure 10a), and 17 malignant cases out of 25 cases (68% of all the cases) in MLO view (Figure 10b) are found to be inside the quadrilateral region. However, only 7 benign cases out of 33 cases (21% of all the cases) in CC view

and only 4 benign cases out of 33 cases (12% of all the cases) in MLO view are found to be inside the quadrilateral region. This difference in region preference shows that there is a correlation between the Hurst value of the background tissue and the fractal dimension value of MC clusters to differentiate benign cases from malignant cases.

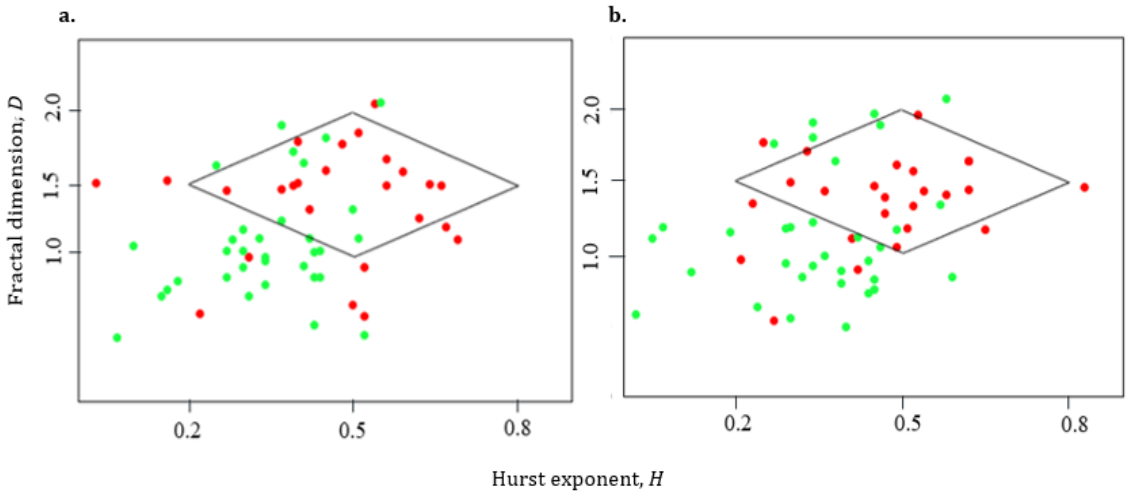

Figure 10: Fractal dimension vs Hurst exponent shown for both CC (a) and MLO (b) indicates the correlation between H and D in differentiating benign MC (green) from malignant MC (red). The identified quadrilateral region is centered at [0.5,1.5] and it extends horizontally between $0.2<H<0.8$ and vertically between $1.0<D<2.0$. The benign MC have a preference to reside outside the quadrilateral region, whereas the malignant MC have a preference to reside in the inside of the quadrilateral region.

In the 2014 paper the "2D CC-MLO fractal dimension plot", as shown here in Figure 8, was graphed to demonstrate the relationship between malignant and benign cases when D from the MLO view is plotted as a function of D from the CC view. Following the graphical analysis from Figure 10, we also graphed a 2D scatter plot just for the Hurst exponent, H, obtained for both benign and malignant cases, where H from MLO view is plotted as a function of CC view, as shown in Figure 11a. A box plot is then used to show the distribution of benign and malignant cases in both CC view (Figure 11b) and MLO view (Figure 11c). In the 2D scatter plot shown in Figure 10a, if we consider the central

point (0.5,0.5), according to the box plots in Figure 11b and 11c, ~75% of the malignant cases (red dots) are located near the (0.5,0.5) region with the median of $H \sim 0.5$. On the other hand, again from the box plots analysis in Figure 11b and 11c, ~75% of the benign cases (green dots) are located near the coordinate (0.36,0.36) with median of $H \sim 0.36$. Then *p*-value was evaluated using the nonparametric Wilcoxon rank sum test for a statistical comparison between the Hurst values of benign and malignant cases. The *p*-value obtained for *H*(CC) is 0.00257 (<0.05) and *p*-value obtained for *H*(MLO) is 0.00544 (<0.05) which shows that there is a statistically significant difference between Hurst values of benign and malignant cases. The observation of the Hurst exponent, *H*, scatter plot and the box plot analysis in Figure 11, and the *p*-values for *H*, indicates that background breast tissue microenvironment surrounding microcalcification has some disruption. This can also be confirmed by the outcome from the 2017 study as the median value $H \sim 0.5$ is in the range $0.45<H<0.55$ which is identified to be disrupted tissue region.[13]

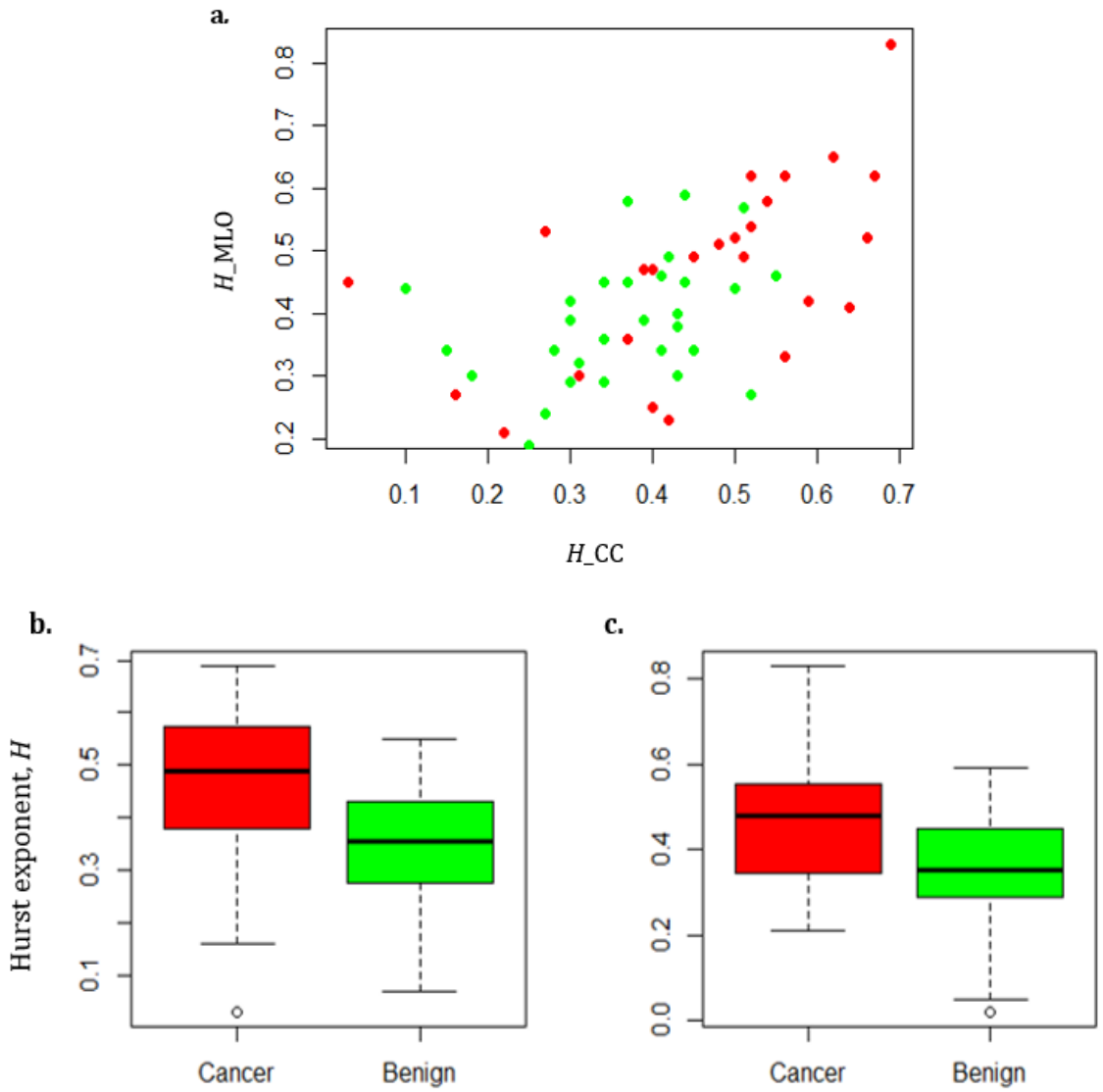

Figure 11: The 2D scatter plot (a.) represents the Hurst value, *H*, from MLO view plotted as a function of *H* from CC view for benign MC (green dots) and malignant MC (red dots). The two box plots for CC view (b.) and MLO view (c.) show that malignant cases (red box) have a strong preference of median near $H = 0.5$ unlike benign cases (green box).

We calculated a new variable denoted generally as, *Z*. This new variable represents the distance calculated for each Hurst exponent, *H,* of benign and malignant cases from two radial centers in the *H*(MLO) vs. *H*(CC) plot shown in Figure 9a: (0,0) and (0.5,0.5) using the distance equation.

$$Z = \sqrt{((x_1 - x_2)^2 + (y_1 - y_2)^2)} \qquad \text{Eq. 4}$$

These two radial centers are chosen to analyze the behavior of both malignant and benign cases between 0-0.5 as this range of Hurst is an indicator of anti-persistent (anti-correlation) behavior. The variables are calculated for CC and MLO views separately. The Z calculated from the center point (0.5,0.5) is denoted as $Z_{0.5}$, and the Z calculated from the center point (0,0) is denoted as $Z_{0.0}$. They represent how far away each data points for benign and malignant cases are from each center points. The box plots shown in Figures 12A and 12B are used to statistically analyze differences between malignant and benign cases for each variables $Z_{0.0}$ and $Z_{0.5}$ respectively. Then the p-value was evaluated using the nonparametric Wilcoxon rank sum test in R to statistically compare the obtained values of $Z_{0.0}$ and $Z_{0.5}$ for benign and malignant cases.

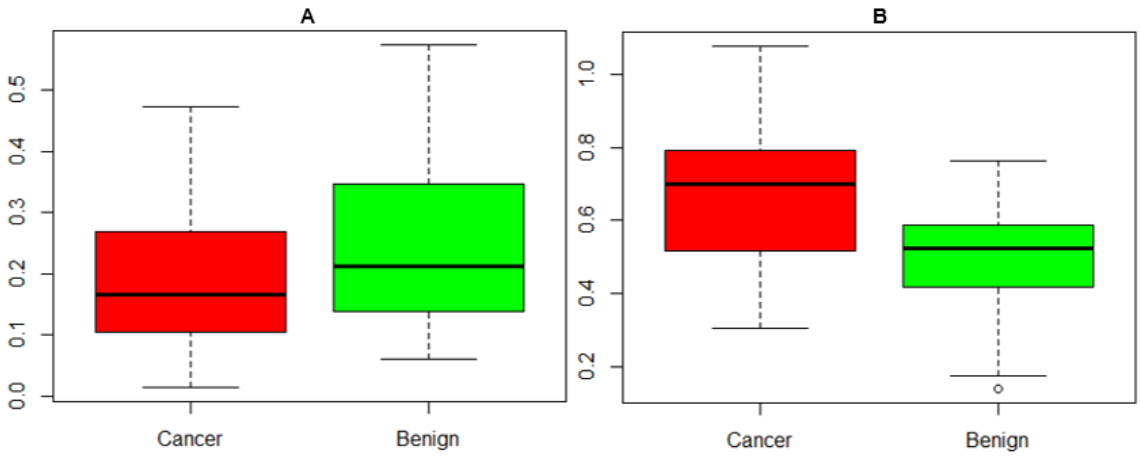

Figure 12: A box plot representing the statistical difference between $Z_{0.5}$ (**A**) and $Z_{0.0}$ (**B**) for both benign cases (green box) and malignant cases (red box).

The box plot in Figure 12 compares the distance $Z_{0.0}$ and $Z_{0.5}$ calculated for both benign (green box) and malignant cases (red box). The median of $Z_{0.5}$, for benign cases is 0.1664 whereas the median for malignant cases is 0.2126. The median for $Z_{0.0}$, for benign cases is 0.5243 whereas the median for malignant cases is 0.7004. The median of benign cases is greater than the median of malignant cases for $Z_{0.5}$, however, the median for benign

cases is less than the median of malignant cases for $Z_{0.0}$. These median values show that there exists a difference between the benign cases and malignant cases in terms of choosing a region to reside. The *p*-value for $Z_{0.5}$ is 0.1634 (>0.05) which shows that there is no statistically significant difference between the distance of each data point from the center for both benign and malignant cases. Whereas the *p*-value for $Z_{0.0}$ is 0.001066 (<0.05) which shows that there is a statistically significant difference between the distance of benign and malignant cases from the center (0,0). These statistical results are indicators such that when the 3D graph for *D* vs *H* is plotted, there is an expectation for more malignant cases (red dots) to be near 0, the origin and more benign cases (green dots) to be far away from the origin. In addition, the statistical analysis of the box plot in R showed that 75% of the malignant cases have $Z_{0.0} < 0.7844$ and $Z_{0.5} < 0.2599$, and 75% of the benign cases have $Z_{0.0} < 0.5872$ and $Z_{0.5} < 0.3471$. Based on these results, when the 3D graph for Hurst exponent vs fractal dimension is plotted, one can expect to see relatively more benign cases far away from the origin for $Z_{0.5}$ and more malignant cases near the origin for $Z_{0.0}$. The closer the *H* values are to 0, the stronger is the tendency for the time series to revert to its long term means value. This means that there is tissue disruption in the microenvironment of breast surrounding malignant MC clusters. This analysis also indicates the quantifiable relationship between the Hurst exponent quantifying tissue disruption and fractal dimension of MC clusters in differentiating between benign and malignant cases. However, there is a need for further analysis of this relationship with more data to make a conclusion confirming the presence of tissue disruption in all malignant MC clusters that could be applied for a reliable diagnostic process.

Next, we wanted to combine the information on the x and y from the 2D CC-MLO Hurst exponent plot with the 2D CC-MLO fractal dimension plot from 2014 (Figure 8). Together this created 4-dimensional data information. However, since a 4-dimensional plot is not possible to graph, we instead decided to consider the information in a 3D plot combining D(CC), D(MLO), and Z as shown in Figure 13. To do so, we used the fractal dimension D for CC to go in the x-axis, D from the MLO view to go in the y-axis, and the variables $Z_{0.0}$ and the $Z_{0.5}$, respectively, to go in the z-axis. The two variables $Z_{0.0}$ and $Z_{0.5}$, calculated above represent the combined Hurst exponent, H, from CC and MLO views for benign and malignant cases. Two separate graphs one with $Z_{0.0}$ in the z-axis and another with $Z_{0.5}$ in the z-axis but, with same D from CC and D from MLO was used to graph the "3D CC-MLO fractal dimension vs Hurst exponent" plots, as shown in Figure 13. Although there is not a clear pattern that the data points follow, the 3D plots in Figure 13 demonstrates the 4-dimensional information relating the Hurst exponent, H, and fractal dimension, D, of benign and malignant cases from both CC and MLO views. No statistical analyses were performed on these 3D data, but we qualitatively observed that there seem to be a relationship between the Hurst exponent, H, quantifying the disruption in the surrounding breast tissue and the fractal dimension, D, showing the fractality of the MC clusters.

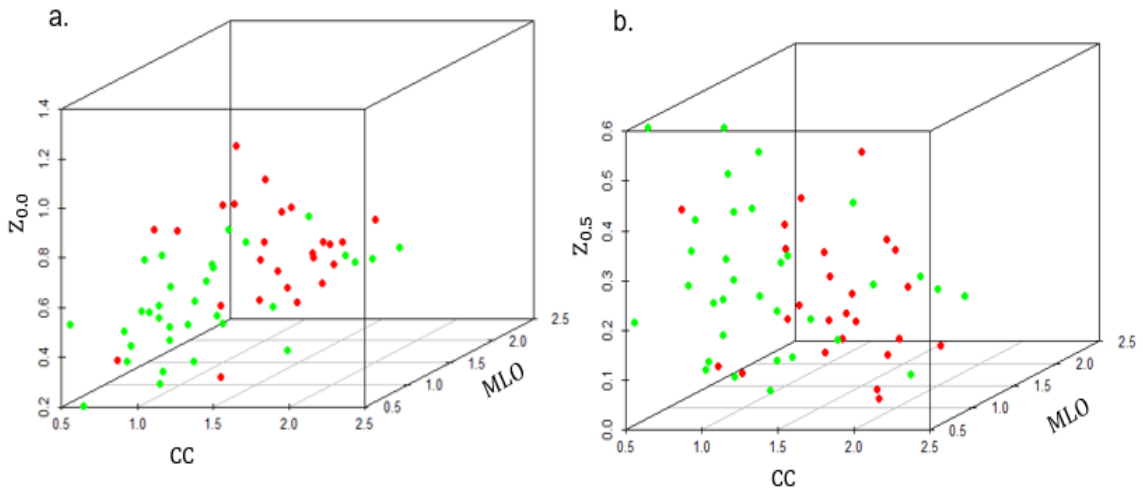

Figure 13: 3D plot of D from CC (x-axis) and MLO (y-axis) against the variable $Z_{0.0}$, (**a)**, and $Z_{0.5}$ (**b).**

CHAPTER 6: CONCLUSION

Microcalcifications inside the breast tissue sometimes grow into a cancerous tumor. The identification, characterization and quantification of MC clusters when analyzing mammograms is very useful for early cancer detection. In a previous study done by CompuMAINE Lab in 2014, mammograms were analyzed with the aid of the 2D WTMM method and it was found that malignant MC clusters have a fractal nature. The microenvironment surrounding these MC clusters also plays a role in identification of suspicious areas leading to possible cancerous tumor growth. A separate study done by this same team in 2017 used the 2D WTMM method to analyze mammograms which showed that the loss of tissue homeostasis in the breast microenvironment leading to tissue disruption can be quantified by the global roughness exponent, H.[13] The results from this study has found that the Hurst value for a disrupted tissue region is between $0.45<H<0.55$.

In this project the correlation between the Hurst exponent value for the background tissue surrounding MC clusters and the fractal dimension of MC clusters was studied. In the "2D fractal dimension vs. Hurst exponent plot" nearly 75% of the malignant cases are found inside the quadrilateral region centered at the point (0.5,1.5). Since $H \sim 0.5$ is associated with a disrupted tissue region and $D \sim 1.5$ is associated with malignant MC clusters, we can conclude that there is a relationship between the state of the microenvironment in cancerous breast tissue and microcalcifications clustering in that region. The 3D graph in Figure 13 is an additional supporting evidence for this relationship. As a conclusion, based on the outcomes of this study one can hypothesize that with further analyses, loss of tissue homeostasis describing the state of the microenvironment of a breast

tissue and the fractal nature of MC clusters have a quantifiable relationship to distinguish benign cases from malignant cases in mammogram analysis. This outcome also leads to a future work that can be employed to distinguish whether it is the tissue disruption as a result of loss of tissue homeostasis that is facilitating the growth of microcalcification clusters or vice-versa.

REFERENCES

1. Kriege, M. *et al.* Efficacy of MRI and mammography for breast-cancer screening in women with a familial or genetic predisposition. *N. Engl. J. Med.* (2004). doi:10.1056/NEJMoa031759

2. Huo, Z. *et al.* Computerized analysis of digitized mammograms of BRCA1 and BRCA2 gene mutation carriers. *Radiology* (2002). doi:10.1148/radiol.2252010845

3. Morris, E. A. Review of breast MRI: Indications and limitations. *Seminars in Roentgenology* (2001). doi:10.1053/sroe.2001.25123

4. Orel, S. G. & Schnall, M. D. MR imaging of the breast for the detection, diagnosis, and staging of breast cancer. *Radiology* (2001). doi:10.1148/radiology.220.1.r01jl3113

5. Gur, D. *et al.* Changes in breast cancer detection and mammography recall rates after the introduction of a Computer-aided detection system. *J. Natl. Cancer Inst.* (2004). doi:10.1093/jnci/djh067

6. Mandelson, M. T. Breast Density as a Predictor of Mammographic Detection: Comparison of Interval- and Screen-Detected Cancers. *J. Natl. Cancer Inst.* (2000). doi:10.1093/jnci/92.13.1081

7. Batchelder, K. A. *et al.* Wavelet-based 3D reconstruction of microcalcification clusters from two mammographic views: New evidence that fractal tumors are malignant and euclidean tumors are benign. *PLoS One* (2014). doi:10.1371/journal.pone.0107580

8. Bizzarri, M. *et al.* Fractal analysis in a systems biology approach to cancer. *Seminars in Cancer Biology* (2011). doi:10.1016/j.semcancer.2011.04.002

9. Kahn, E. & Paola, R. Di. A Fractal Approach to the Segmentation of Microcalcifications in Digital Mammograms. *Med. Phys.* (1995). doi:10.1118/1.597473

10. Li, H., Liu, K. J. R. & Lo, S. C. B. Fractal modeling and segmentation for the enhancement of microcalcifications in digital mammograms. *IEEE Trans. Med. Imaging* (1997). doi:10.1109/42.650875

11. Sankar, D. & Thomas, T. A new fast fractal modeling approach for the detection of microcalcifications in mammograms. *J. Digit. Imaging* (2010). doi:10.1007/s10278-009-9224-6

12. Hergarten, S. *Self-Organized Criticality in Earth Systems*. *Self-Organized Criticality in Earth Systems* (2002). doi:10.1007/978-3-662-04390-5

13. Marin, Z. *et al.* Mammographic evidence of microenvironment changes in tumorous breasts: *Med. Phys.* (2017). doi:10.1002/mp.12120

14. Geddes, D. T. Inside the Lactating Breast: The Latest Anatomy Research. *J. Midwifery Women's Heal.* (2007). doi:10.1016/j.jmwh.2007.05.004

15. Johnson, M. C. Anatomy and physiology of the breast. in *Management of Breast Diseases* (2010). doi:10.1007/978-3-540-69743-5_1

16. Kovacs, C. S. Calcium and bone metabolism disorders during pregnancy and lactation. *Endocrinology and Metabolism Clinics of North America* (2011). doi:10.1016/j.ecl.2011.08.002

17. Carmeliet, G., Van Cromphaut, S., Daci, E., Maes, C. & Bouillon, R. Disorders of calcium homeostasis. *Best Practice and Research: Clinical Endocrinology and Metabolism* (2003). doi:10.1016/j.beem.2003.08.001

18. Hoey, R. P. *et al.* The parathyroid hormone-related protein receptor is expressed in breast cancer bone metastases and promotes autocrine proliferation in breast carcinoma cells. *Br. J. Cancer* (2003). doi:10.1038/sj.bjc.6600757

19. Almquist, M., Manjer, J., Bondeson, L. & Bondeson, A. G. Serum calcium and breast cancer risk: Results from a prospective cohort study of 7,847 women. *Cancer Causes Control* (2007). doi:10.1007/s10552-007-9001-0

20. Wilkinson, L., Thomas, V. & Sharma, N. Microcalcification on mammography: Approaches to interpretation and biopsy. *British Journal of Radiology* (2017). doi:10.1259/bjr.20160594

21. Castellaro, A. M. *et al.* Oxalate induces breast cancer. *BMC Cancer* (2015). doi:10.1186/s12885-015-1747-2

22. Breastcancer.org. Understanding Breast Calcifications. *BREASTCANCER.ORG*

23. Nalawade, Y. V. Evaluation of breast calcifications. *Indian J. Radiol. Imaging* (2009). doi:10.4103/0971-3026.57208

24. Park, J. M. *et al.* Clustering of breast microcalcifications: Revisited. *Clin. Radiol.* (2000). doi:10.1053/crad.1999.0220

25. WHO. WHO | Breast cancer. (2018).

26. Ferlay, J. *et al.* GLOBOCAN 2012 v1.0, Cancer Incidence and Mortality Worldwide: IARC CancerBase. No. 11 [Internet]. *Lyon, France: IARC* (2013).

27. Sankaranarayanan, R. *et al.* Cancer survival in Africa, Asia, and Central America: a population-based study. *Lancet Oncol.* (2010). doi:10.1016/S1470-2045(09)70335-3

28. Corbex, M., Bouzbid, S. & Boffetta, P. Features of breast cancer in developing countries, examples from North-Africa. *European Journal of Cancer* (2014). doi:10.1016/j.ejca.2014.03.016

29. Eerola, H., Blomqvist, C., Pukkala, E., Pyrhönen, S. & Nevanlinna, H. Familial breast cancer in southern Finlandhow prevalent are breast cancer families and can we trust the family history reported by patients? *Eur. J. Cancer* (2000). doi:10.1016/S0959-8049(00)00093-9

30. Ewertz, M. *et al.* Age at first birth, parity and risk of breast cancer: A meta-analysis of 8 studies from the nordic countries. *Int. J. Cancer* (1990). doi:10.1002/ijc.2910460408

31. Hamajima, N. *et al.* Alcohol, tobacco and breast cancer - Collaborative reanalysis of individual data from 53 epidemiological studies, including 58 515 women with breast cancer and 95 067 women without the disease. *Br. J. Cancer* (2002). doi:10.1038/sj.bjc.6600596

32. Shulman, L. N., Willett, W., Sievers, A. & Knaul, F. M. Breast cancer in developing countries: Opportunities for improved survival. *J. Oncol.* (2010). doi:10.1155/2010/595167

33. Ferlay J, Shin HR, Bray F, Forman D, Mathers C, Parkin D, . Estimates of worldwide burden of cancer in 2008: GLOBOCAN 2008. International journal of cancer. *Int. J. Cancer* (2010).

34. Ngoma, T. A. World Health Organization cancer priorities in developing countries. *Annals of Oncology* (2006). doi:10.1093/annonc/mdl982

35. Denny, L. *et al.* Interventions to close the divide for women with breast and cervical cancer between low-income and middle-income countries and high-income countries. *The Lancet* (2017). doi:10.1016/S0140-6736(16)31795-0

36. Lauby-Secretan, B. *et al.* Breast-cancer screening-viewpoint of the IARC working group. *N. Engl. J. Med.* (2015). doi:10.1056/NEJMsr1504363

37. Papavramidou, N., Papavramidis, T. & Demetriou, T. Ancient greek and greco-Roman methods in modern surgical treatment of cancer. *Annals of Surgical Oncology* (2010). doi:10.1245/s10434-009-0886-6

38. Shapiro, S., Strax, P. & Venet, L. Periodic Breast Cancer Screening in Reducing Mortality From Breast Cancer. *JAMA J. Am. Med. Assoc.* (1971). doi:10.1001/jama.1971.03180240027005

39. Siu, A. L. Screening for breast cancer: U.S. Preventive services task force recommendation statement. *Annals of Internal Medicine* (2016). doi:10.7326/M15-2886

40. Van Steen, A. & Van Tiggelen, R. Short history of mammography: A Belgian perspective. *Journal Belge de Radiologie* (2007).

41. Pisano, E. D. *et al.* Diagnostic performance of digital versus film mammography for breast-cancer screening. *N. Engl. J. Med.* (2005). doi:10.1056/NEJMoa052911

42. Gold, R. H. The evolution of mammography. *Radiologic Clinics of North America* (1992).

43. GOULD, H. R., RUZICKA, F. F., SANCHEZ-UBEDA, R. & PEREZ, J. Xeroradiography of the breast. *Am. J. Roentgenol. Radium Ther. Nucl. Med.* (1960).

44. Verma, B. & Zakos, J. A computer-aided diagnosis system for digital mammograms based on fuzzy-neural and feature extraction techniques. *IEEE Trans. Inf. Technol. Biomed.* (2001). doi:10.1109/4233.908389

45. Sweeney, R. J. I., Lewis, S. J., Hogg, P. & McEntee, M. F. A review of mammographic positioning image quality criteria for the craniocaudal projection.

British Journal of Radiology (2018). doi:10.1259/bjr.20170611

46. Popli, M. B., Teotia, R., Narang, M. & Krishna, H. Breast positioning during mammography: Mistakes to be avoided. *Breast Cancer Basic Clin. Res.* (2014). doi:10.4137/BCBCr.s17617

47. Suri, J. S. & Rangayyan, R. M. *Recent advances in breast imaging, mammography, and computer-aided diagnosis of breast cancer*. *Recent Advances in Breast Imaging, Mammography, and Computer-Aided Diagnosis of Breast Cancer* (2006). doi:10.1117/3.651880

48. Buchanan, C. L., Morris, E. A., Dorn, P. L., Borgen, P. I. & Van Zee, K. J. Utility of breast magnetic resonance imaging in patients with occult primary breast cancer. *Ann. Surg. Oncol.* (2005). doi:10.1245/ASO.2005.03.520

49. Gilbert, F. J. *et al.* Single reading with computer-aided detection for screening mammography. *N. Engl. J. Med.* (2008). doi:10.1056/NEJMoa0803545

50. Fenton, J. J. *et al.* Influence of computer-aided detection on performance of screening mammography. *N. Engl. J. Med.* (2007). doi:10.1056/NEJMoa066099

51. Fenton, J. J. *et al.* Effectiveness of computer-aided detection in community mammography practice. *J. Natl. Cancer Inst.* (2011). doi:10.1093/jnci/djr206

52. Noble, M., Bruening, W., Uhl, S. & Schoelles, K. Computer-aided detection mammography for breast cancer screening: Systematic review and meta-analysis. *Arch. Gynecol. Obstet.* (2009). doi:10.1007/s00404-008-0841-y

53. Fenton, J. J. *et al.* Short-term outcomes of screening mammography using computer-aided detection a population-based study of medicare enrollees. *Ann. Intern. Med.* (2013). doi:10.7326/0003-4819-158-8-201304160-00002

54. Eadie, L. H., Taylor, P. & Gibson, A. P. A systematic review of computer-assisted diagnosis in diagnostic cancer imaging. *Eur. J. Radiol.* (2012). doi:10.1016/j.ejrad.2011.01.098

55. Kim, S. J., Moon, W. K., Seong, M. H., Cho, N. & Chang, J. M. Computer-aided detection in digital mammography: False-positive marks and their reproducibility in negative mammograms. *Acta radiol.* (2009). doi:10.3109/02841850903216700

56. C.D., L. *et al.* Diagnostic accuracy of digital screening mammography with and

without computer-aided detection. *JAMA Intern. Med.* (2015). doi:10.1001/jamainternmed.2015.5231 LK -

57. Khalil, A., Joncas, G., Nekka, F., Kestener, P. & Arneodo, A. Morphological Analysis of H i Features. II. Wavelet-based Multifractal Formalism . *Astrophys. J. Suppl. Ser.* (2006). doi:10.1086/505144

58. MUZY, J. F., BACRY, E. & ARNEODO, A. THE MULTIFRACTAL FORMALISM REVISITED WITH WAVELETS. *Int. J. Bifurc. Chaos* (1994). doi:10.1142/s0218127494000204

59. Lin, D. C. & Sharif, A. Wavelet transform modulus maxima based fractal correlation analysis. *Eur. Phys. J. B* (2007). doi:10.1140/epjb/e2008-00004-6

60. Arneodo, A., Bacry, E. & Muzy, J. F. The thermodynamics of fractals revisited with wavelets. *Phys. A Stat. Mech. its Appl.* (1995). doi:10.1016/0378-4371(94)00163-N

61. Arneodo, A., Audit, B., Kestener, P. & Roux, S. Wavelet-based multifractal analysis. *Scholarpedia* (2008). doi:10.4249/scholarpedia.4103

62. Arnéodo, A., Decoster, N., Kestener, P. & Roux, S. G. A wavelet-based method for multifractal image analysis: From theoretical concepts to experimental applications. *Adv. Imaging Electron Phys.* (2003). doi:10.1016/S1076-5670(03)80014-9

63. Gerasimova, E. *et al.* Wavelet-based multifractal analysis of dynamic infrared thermograms to assist in early breast cancer diagnosis. *Front. Physiol.* (2014). doi:10.3389/fphys.2014.00176

64. Kestener, P., Lina, J. M., Saint-Jean, P. & Arneodo, A. WAVELET-BASED MULTIFRACTAL FORMALISM TO ASSIST IN DIAGNOSIS IN DIGITIZED MAMMOGRAMS. *Image Anal. Stereol.* (2011). doi:10.5566/ias.v20.p169-174

65. Khalil, Andre, K. A. B. Improved Methods of Cancer Detection.

66. R Core Team. R: A Language and Environment for Statistical Computing. *R Foundation for Statistical Computing* (2013). Available at: http://www.r-project.org/.

AUTHOR'S BIOGRAPHY

Betelhem was born in Addis Ababa, Ethiopia in 1998. She was raised in the capital city of Ethiopia, Addis Ababa. She finished her primary, secondary, and Highschool in Nativity Girls' School, a Catholic missionaries school located in Piassa, a town in the capital city. She graduated from her Highschool on July 23, 2016 and came to the University of Maine with a scholarship to study Biology on January 10, 2017. Due to her passion in integrating mathematics with her Biological study, she has switched her major to Biomedical Engineering. Since her second year she has been involved in different research labs like the Virtual Environmental and Multimodal Interaction Laboratory (VEMI Lab), CompuMAINE Lab, and Dr. Han's Genetics Lab. She also participated in Team Maine as a student ambassador in the Admissions Office, and other student organizations like the African Student Association where she served as a president, International Student Association, Bioengineering club, Society of Women Engineers where she served as the social chair. She has also been inducted to All Maine Women, a traditional honors society at UMaine, in recognition of her hard work, Maine spirit, good academic standing, and community service to UMaine community. She has received the International Presidential Scholarship and Richard E. Durst Scholarship due to her academic excellence. Her undergraduate independent study has also been awarded the Carolyn E. Reed Pre-Medical Studies Honors Thesis Fellowship and Charlie Slavin Research Fund.

After finishing her Bachelor of Science in Biomedical engineering she plans to work as a research assistant in a biological research laboratory and further pursue her education to Master of Science and PhD. She aims to do her M.Sc and PhD on the

application of imaging in point of care disease diagnostics for several chronic, genetic, and hereditary diseases.